crystals

MDPI

Article

Effect of Prewetting Cenospheres on Hydration Kinetics, Microstructure, and Mechanical Properties of Refractory Castables

Ina Pundienė * and Jolanta Pranckevičienė

Institute of Building Materials, Vilnius Gediminas Technical University, Saulėtekio al. 11, 10223 Vilnius, Lithuania; jolanta.pranckeviciene@vilniustech.lt

* Correspondence: ina.pundiene@vilniustech.lt

Abstract: This study investigated the effect of non-prewetted and prewetted cenospheres (CSs) on the hydration course and physical and mechanical properties of refractory castable mixtures incorporated with nano silica (NS). The fixed amount of 0.1% of NS improves the compressive strength of the refractory castable, containing various proportions of non-prewetted and prewetted CSs (up to 25% in composition). It was found that an increase in CSs slows down the hydration of cement and the early structure formation of refractory castable mixtures. Proportionally, due to the increase in the amount of non-prewetted and prewetted CSs in the composition, the density of the samples decreases from 1875 kg/m^3 to 1310 kg/m^3 after firing. The amount of CSs varied from 15 to 25% in the composition, increasing compressive strength by up to 5.3% and 8.6% in the case of non-prewetted CSs and by up to 39.2% and 20.5% in the case of prewetted CSs after the drying process. Prewetting CSs provides additional internal water that facilitates cement hydration during drying, promoting the formation of stratlingite (C_2ASH_8), a key hydration product that enhances mechanical properties after firing and promotes the early formation of anorthite. The firing at 800 °C and 1100 °C temperatures decreases compressive strength to a greater extent, as more CSs are in the composition. However, prewetting of CSs leads to significantly less deterioration (up to 32%, compared to compositions with non-prewetted CSs) in the compressive strength of refractory castables. The shrinkage of the refractory castable samples after firing at 1100 °C reached 0.16% in the case of non-prewetted CSs and 0.1% in the case of prewetted CSs. Prewetted CSs in refractory castables relaxes the stresses arising during firing more efficiently and practically compensates for shrinkage processes.

Keywords: cenospheres; prewetting; aluminate cement; hydration; stratlingite; compressive strength

check for updates

Academic Editor: Vladislav V. Gurzhiy

Received: 11 December 2024
Revised: 6 January 2025
Accepted: 10 January 2025
Published: 12 January 2025

Citation: Pundienė, I.; Pranckevičienė, J. Effect of Prewetting Cenospheres on Hydration Kinetics, Microstructure, and Mechanical Properties of Refractory Castables. *Crystals* **2025**, *15*, 68. https://doi.org/10.3390/cryst15010068

Copyright: © 2025 by the authors. Licensee MDPI, Basel, Switzerland. This article is an open access article distributed under the terms and conditions of the Creative Commons Attribution (CC BY) license (https://creativecommons.org/licenses/by/4.0/).

1. Introduction

Refractory castable technology can solve many issues, including controlling the rheological properties of the mix, lowering aluminate cement consumption, and enhancing the mechanical and physical qualities of castables by adjusting the properties of refractory castables using fillers based on waste products that are appropriate in chemical composition. Along with technology, it solves additional ecological problems related to waste management and reduces the use of aluminate cement, which significantly impacts nature. Lightweight refractory castables designed for high-temperature applications offer significant advantages in industries such as metallurgy, power generation, and cement

manufacturing. Castables resistant to high temperatures can be placed into intricately shaped structures [1].

Aluminosilicate microspheres, also known as cenospheres (CSs), are a less developed filler in the fabrication of refractory castables [2]. They are formed along with heavier ash when coal, oil, wood, and domestic waste are burned [3,4]. CSs are one of fly ash's most important value-added materials [5]. The gathered ashes contaminate the environment by piling up in landfills. Because aluminosilicate CSs are hollow spheres, are the lightest component, and often have a very low bulk density (0.3–0.5 g/cm^3), they tend to form deposits on the ash layer's surface in settling tanks [5,6].

Despite their hollow and lightweight structure, CSs possess impressive mechanical properties, including compressive strength ranging from 70 MPa to 140 MPa and a Mohs hardness of 6–7, attributed to their durable aluminosilicate shells [7]. The outstanding insulation properties of CSs (thermal conductivity varies between 0.1 W/m·K and 0.2 W/m·K) enable their use in today's technologies. The incorporation of CSs enhances the flow characteristics of pastes due to their spherical shape, while their chemical inertness to acids and alkalis and high thermal stability (typically stable between 1000 °C and 1450 °C) make them suitable for refractory applications [8–10]. They can also be utilised to create ultra-lightweight cement-based composites (ULCC) that are strong and have low heat conductivity [11].

Concrete made with Portland cement is known to incorporate CSs successfully. In order to produce Portland cement with novel qualities and at a reduced cost, CSs have recently been added to the composition of Portland cement during the production stage [12]. CS application improves monolithic linings' placability by giving the product superior flow characteristics. This behaviour has been attributed to the spherical particles' lubricating (ball-bearing) properties. A partial replacement of normal-weight aggregate by 25% by volume of saturated lightweight aggregate effectively eliminated the self-induced shrinkage and internal stress development of the normal-weight concrete. It should be noted that the internal water supply from the saturated lightweight aggregate to the high-strength cement matrix caused continuous expansion, which may be related to the continuous hydration effect [13].

CSs, as micro-aggregates, were discovered in research [14] to be an excellent way to introduce voids while lowering the density and thermal conductivity of ultra-lightweight cement composites. The CS's spherical shape promotes the concrete's strength and lowers the heat of hydration [3,15,16]. Only a 10% replacement of pumice LW aggregate to cenospheres can increase the compressive strength of lightweight concrete. Higher replacement levels (up to 50%) significantly decrease compressive strength [17].

While incorporated into the composition, cenospheres' physical and chemical characteristics are favourable for the production of insulating refractories. The unique characteristics of CSs create numerous opportunities for their use in composite materials, refractory castables and high-temperature ceramics [3]. Another investigation has presented results of using cenospheres (28% in composition) and a small amount of PVA fibre (0.2% and 0.5% in volume) in ultra-lightweight cement composite. After being subjected to elevated temperatures up to 1000 °C, the composite possesses a density of less than 1400 kg/m^3 and a strength of up to 4.6 MPa [18]. Microcracking in the cement paste surrounding the cenosphere particles intensifies as the temperature exceeds 800 °C. SEM analysis shows that because of the cenosphere porous structure and interconnected pores and small channels in the matrix created after the PVA fibres burning, the pore pressure inside ULCC releases.

CSs can be successfully added to different refractory materials to improve thermal characteristics and create lightweight refractory materials. CSs can be used in the production of ceramic [3,19] composite foam materials [20–22] or refractory castables [23–25] due

to their reduced thermal expansion properties. Ceramic foams are suitable for producing high-performance products like heat insulators, thermal resistors, and others since they are lightweight, strong, resistant to gas erosion, and can be moulded into desired shapes [26].

CS-based insulating refractories provide outstanding strength-to-density ratios [27], superior resilience to thermal shock, and an enhanced thermal conductivity-to-bulk density ratio. Despite their relatively low cool pounding quality, they can bear 30 cycles, which are then again heated to 1100 °C and cooled to 25 °C, without exasperating their structural integrity [28,29]. Above all, CS products are significantly more affordable than competing products. The formulation of an individual CS in refractory determines its characteristics. On average, a higher percentage of CS content results in reduced density and better insulating performance. However, the compressive strength decreases significantly when the CS content increases in refractories' composition, even though a CS's solid wall lessens the strength and elastic modulus reductions induced by the lightweight refractory concrete samples' raised porosity [13,30,31]. The use of CSs in heat-insulating or lower-temperature refractories is limited by the maximum service temperature, which is roughly up to 1400 °C [30]. Low-shrinkage refractories are produced by carefully selecting the CS's particle size distribution, which provides ideal particle packing [32].

Notwithstanding their many positive attributes, lightweight refractory castables exhibit some cracking, typically depending on castable characteristics and thermal treatment peculiarities, such as thermal stresses and heating rate. As the firing temperature rises, thermal degradation and crack development for lightweight refractory castables increase [33]. Stress concentrations have been identified in the shell layer of the CS, according to stress distributions in lightweight refractory castables with and without CSs [34]. These studies show that additional strengthening of the contact zone between a CS and the cement matrix is necessary [35]. Various methods have been explored to enhance the strength development of the CS–cement system, such as mechanical treatment, alkali or sulfate activation, or high-temperature treatment [36].

For this purpose, some CS pretreatment methods, such as pre-soaking, water-soaking, and vacuum-soaking, can be promising [37]. The lightweight aggregates absorb more water than typical aggregates. Because of their internal voids and low weight, lightweight aggregates can readily absorb the mixture's water or float while being mixed. From this point of view, prewetting can positively influence the mixture's workability [38]. However, such cases are also possible when dry cement particles form a thin paste coating around the aggregate surface during contact with wet aggregates. The water-to-cement ratio in such coating is lower than in concrete paste, and it can lower the compressive strength of the concrete [39].

Prewetting is a typical procedure for lightweight or porous aggregates before mixing. Prewetting aggregates effectively reduces their absorption potential, enhancing workability. However, its application in field conditions can be more challenging compared to conventional aggregates due to the need for precise water content adjustments [40]. When the water percentage was appropriately calculated to consider the water absorbed by the aggregate prior to mixing, prewetted lightweight aggregate might produce the desired result. The most common practices are applying dry aggregates with water added during mixing or using additional water for prewetting (compared to the reference mixture).

By controlling the water/cement (W/C) ratio, the recycled mortar aggregate prewetting process reduces the water needed when creating new mixtures. The adhesive values of the 20% substitution of recycled aggregate mortar pre-wetted to 67% of its absorption capacity were higher than those of the reference mortar [41]. It has been found that prewetting the recycled aggregate increases strength by about 25% for a 20% substitution of recycled aggregate content. That is in contrast to mortar, which uses

aggregates without prewetting. The pre-wetting procedure is a simple performance strategy that is affordable, eco-friendly, and, most importantly, does not require specific equipment. That is because pre-wetting the aggregates before mixing minimises the water transfer between the aggregates and the cement paste, reducing the water needed to attain project consistency and preventing an increase in the W/C ratio.

CSs can be used as a carrier of different substances for composites and concrete [7]. For example, cenospheres soaked with water or phase change materials (PCMs) have been added to concrete to decrease shrinkage and increase samples' thermal energy storage capacity. Up to 71% of the sample's open crack area, which had a crack width of roughly 0.3 mm, self-healed after 28 days of water exposure when 3 wt.% of CSs was introduced in the composition. Flexural strength was restored due to the self-healing properties of CSs, which caused a maximum 41% decrease in water adsorption. The healing products' primary constituents precipitating on the CS surface were $CaCO_3$ and amorphous C-S-H. A similar observation was reported in research [42,43], which concluded that pre-wetting ceramsite aggregate in lightweight concrete increases compressive strength by 30% after 28 days of curing under matching conditions compared to the reference concrete. The positive effect of the prewetted ceramsite on the early-age autogeneous shrinkage can explain this outcome. The primary reason for this is that the presence of pre-wetting lightweight aggregates can encourage the formation of C-S-H gels in the interfacial zone, and as the water desorption of pre-wetting lightweight aggregates increases, so does the interfacial zone's degree of hydration. It helps to improve the microhardness of the interfacial zone by optimising the microstructure, which raises the compressive strength of cement-based materials. The same is very important to improve cement hydration ability when in composition are prewetted aggregates, in terms of using less mixing water or stored water, which gradually enters the cement and improves the hydration process.

The part of CS consist of broken, damaged, or hollow spheres, with holes on the surface of each CS that connect with the sphere's interior. Such CSs can be pre-wetted and used as a water source to improve cement hydration [44,45]. The prewetted CSs solved the problem of industrial waste fly ash disposal and achieved the reuse of waste. At the same time, the process of preparing saturated microporous cenospheres is simple and efficient. It directly utilises the cenospheres with micropores on the surface as a raw material without destroying the cenospheres' structure. In addition, saturated microporous cenospheres can release a large amount of internal curing water when the humidity of the concrete is reduced, which can better solve the effect of autogenous shrinkage of high-strength concrete. To our knowledge, the effect of different degrees of prewetting of CSs on the physical properties of refractory castables has not been reported.

However, because of their chemical and mineralogical composition, cenospheres belong to supplementary cementitious material. Using prewetted cenospheres opens up the possibility of saving on expensive aluminate cement in producing value-added products because prewetting of cenospheres allows an increase in mechanical strength.

Therefore, this work aims to evaluate the possibility of using prewetted CSs in refractory castables to study the effect of different amounts of CSs on the course of cement hydration, changes in the structure during drying and resulting changes in density, strength, shrinkage and porosity, and to determine the optimal amount of CSs in the composition of concrete.

2. Materials and Methods

2.1. Used Materials

Alumina cement "Gorkal-70" is produced in Poland and meets the essential requirements of the EN 14647 standard [46]. The main phases–CA($CaO{\cdot}Al_2O_3$), CA_2($CaO{\cdot}2Al_2O_3$),

$C_{12}A_7$(12CaO·7Al_2O_3), and Al_2O_3–comprise no less than 70% of the composition (Figure 1). Special characteristics are as follows: refractoriness–at least 1630 °C, specific surface according to the Blain method 450 m^2/kg, specific density–3400–3500 kg/m^3; bulk density–1150 kg/m^3, minimum fraction amount 0–63 μm, not less than 88%.

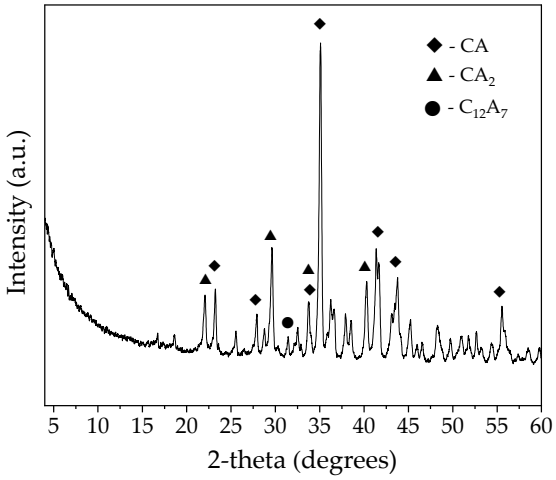


Figure 1. XRD patterns of cement.

Chamotte aggregate (CM) is made by crushing chamotte bricks ($Al_2O_3 \geq 30\%$) with a density of 1920 kg/m^3. The 0/5 mm fractions of chamotte aggregate were used in refractory castables. The bulk density of this fraction of aggregates is 930 kg/m^3.

Ground chamotte (GCM) was also prepared by grinding in a laboratory ball mill. The bulk density of ground chamotte is 1120 kg/m^3, and the specific surface is 0.37 m^2/g.

Nano silica (NS) was produced in "Sigma-Aldrich Chemie GmbH" (Taufkirchen, Germany). Silicon dioxide purity is 99.8% nanopowder, with an average particle size of 12 nm (Figures 2 and 3).

To decrease the composites' water/cement ratio (W/C), deflocculating agents, such as 'Castament FS 20' (PCE-20) from the group of polycarboxylic ethers, are used.

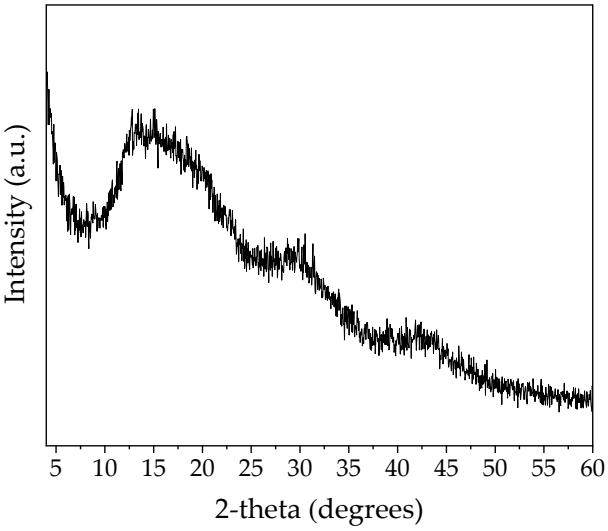


Figure 2. XRD patterns of NS.

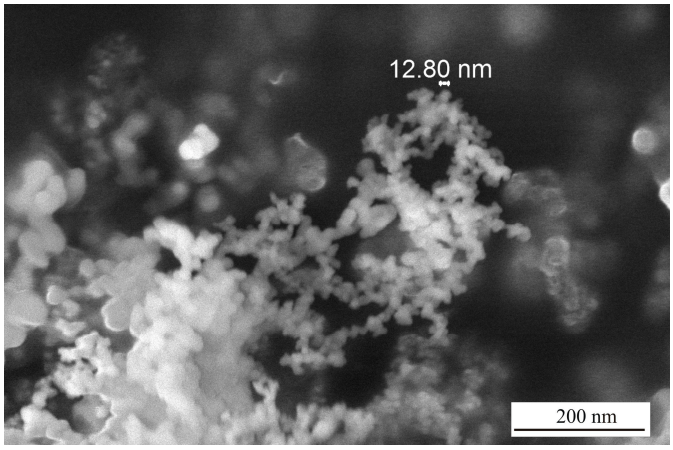


Figure 3. SEM image of NS.

Cenospheres (CSs) were used for research. The chemical (wt.%) and granulometric composition of the CSs used in the studies are presented in Tables 1 and 2. Bulk density is 413 kg/m^3 and the specific surface area of the CSs is 420 m^2/kg. Losses on ignition at a temperature of 400 °C were 0.57%, and at a temperature of 1000 °C the losses were 0.9%. According to the data in Table 2 and Figure 4, the coarser CSs reach 250 μm in diameter, and the surface of coarser spheres is uneven, with many pores and cavities (Figure 5). X-ray phase analysis confirms that the main mineral of the CSs (Figure 6) is mullite ($Al_6Si_2O_{23}$). An amorphous phase was also detected. Although mullite is an inert compound, the amorphous phase may have pozzolanic activity, i.e., the ability to react with cement hydration products.

Table 1. Chemical (wt.%) composition of CSs.

SiO_2	Al_2O_3	Fe_2O_3	CaO	MgO	Na_2O	K_2O
53.8	40.7	1.0	1.4	0.6	0.5	0.4

Table 2. Granulometric composition of CSs.

Residue on a Sieve, (mm) in %							
0.5	0.250	0.125	0.09	0.063	0.045	0.025	>0.025
–	15.6	15.5	56.5	17.0	4.5	1.8	0.2

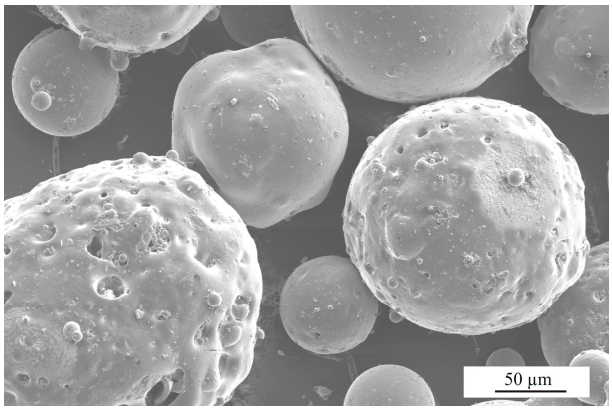


Figure 4. CSs at 100× magnification.

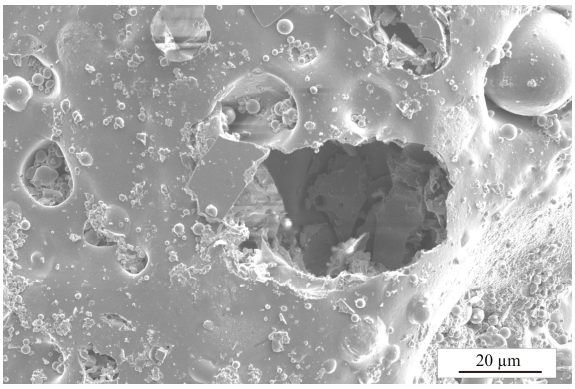


Figure 5. Surface of a CS at 1500× magnification.

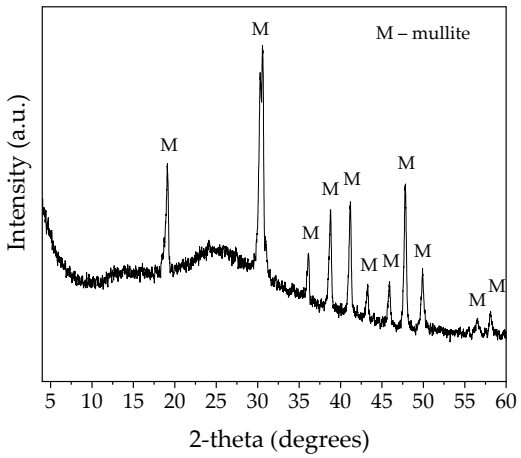


Figure 6. XRD patterns of CSs.

2.2. Mixture Preparation

Prewetted cenospheres were prepared by immersing raw CSs in a 10-L container of water. The mixture was stirred with a paddle for 20 min and allowed to stand for 12 h, following established protocols to ensure uniform saturation. After this time, some of the CSs sank to the bottom, while the rest floated on the water's surface. Only the sunken CSs were collected, drained on a sieve for 30 min, and air-dried for 3 h. The water absorption rate (ω_1) was determined by weighing the prewetted CSs and subjecting them to oven drying at 105 °C for 10 h. The formula used was as follows:

$$\omega_1 = (m_1 - m_2)/m_2 \times 100\%, \quad (1)$$

where ω_1 denotes the water absorption rate, m_1 is the mass of prewetted CS after 3 h of naturally dry up, and m_2 is the mass of CSs after 10 h of drying in the oven.

During the research, the influence of cenospheres (CSs) on the electrical conductivity (EC) and pH of an aqueous solution and the EC and pH of cement pastes with the addition of CSs was determined. To prepare a pure CS suspension, 20 g of CSs was combined with 100 g of distilled water. To prepare pure NS (nano silica) suspension, 0.1 g of NS was mixed with 100 g of distilled water. Cement suspensions were prepared with the following ratios: K-0 (cement:CS ratio 1:0), K-1 (cement:CS ratio 1:0.1), K-2 (cement:CS ratio 1:0.25), K-3 (cement:NS ratio 1:0.01), K-4 (cement:CS:NS ratio 1:0.1:0.01), and K-5 (cement:CS:NS 1:0.25:0.01). EC and pH values were measured at intervals over 20 min to track hydration changes.

Refractory castable mixtures were prepared in a 20-L Hobart forced-mix mixer at room temperature. For non-prewetted CS compositions, the dry components (cement, chamotte

aggregates, and ground chamotte) were mixed for 3 min. Half of the water content (50–60%) was added, and the mixture was mixed for another 3 min. The remaining water was added, and the mixture was mixed for 5 min. For prewetted CS compositions, the dry components were mixed for 3 min, followed by the addition of 30–35% of the total water content, adjusted for water absorbed by the CSs. Prewetted CSs and the remaining water were added, and the mixture was mixed for 5 min. The prepared mixtures were poured into moulds measuring 70 × 70 × 70 mm, compacted under slight vibration, and covered with polyethene sheets. Samples were cured for 72 h at 20 ± 1 °C. The cured samples were dried in an electric furnace at 105 °C for 48 h and fired at 800 °C and 1100 °C in an electronically controlled furnace at a heating rate of 5 °C/h. The samples were held at the peak temperature for 5 h and cooled to room temperature at 60 °C/h.

To study the effect of adding different amounts of CSs and the influence of prewetting CSs on cement hydration and concrete's physical and mechanical properties, 10 compositions with different amounts of CSs were prepared (Table 3). In the first control composition, A-0, only fireclay filler was used, and in composition, A-NS, only fireclay filler and NS additive were used. In the compositions A10–A25 and ANS10–ANS25, the amount of CSs varied from 10% to 25%. However, the CSs in ANS10–ANS25 compositions was prewetted according to the procedure in the methods section of this paper. The increase in the amount of CSs was carried out by reducing the amount of chamotte in the composition.

Table 3. Compositions of refractory concrete with different amounts of CSs, %.

Sample	Used Materials in wt.%								
	B-70	CS	GCM	CM	NS	PCE-20	Water Used in a Mixture over 100 Dry Materials, %	Water Adsorbed in CS%	Total Water Content *
A-0	15	–	35	50	–	0.1	14.8	–	–
A-NS	15	–	35	50	0.1	0.1	14.8	–	–
AS-10	15	10	25	50	0.1	0.1	15.9	–	–
AS-15	15	15	20	50	0.1	0.1	16.8	–	–
AS-20	15	20	15	50	0.1	0.1	19.1	–	–
AS-25	15	25	10	50	0.1	0.1	20.8	–	–
APS-10	15	10	25	50	0.1	0.1	12.4	3.50	15.9
APS-15	15	15	20	50	0.1	0.1	11.6	5.25	16.8
APS-20	15	20	15	50	0.1	0.1	11.9	7.20	19.1
APS-25	15	25	10	50	0.1	0.1	12.55	8.25	20.8

* over 100% dry components.

The amount of water in the compositions increases with the amount of CSs and grows from 14.8% to 20.8% over 100% of the dry components. However, the total amount of water was the same for compositions with dry or prewetted CSs. The water adsorbed by CSs was calculated, and in such a way, water added to dry components was decreased.

For the XRD testing of pure cement matrix (AM-0) and cement matrix with NS addition (AM-NS), samples were prepared. To prepare AM-0, 60 g of cement and 18 g of water were used. To prepare AM-NS, 60 g of cement, 18 g of water and 0.4 g of NS were used. Samples were cured, and the XRD was recorded after 100 °C, 900 °C, 1000 °C, and 1100 °C.

2.3. Methods

During the research, the influence of CSs on the electrical conductivity (EC) and pH of an aqueous solution and the EC and pH of cement pastes with the addition of CSs was determined. Device MPC 227 of the company METTLER TOLEDO (Greifensee,

Switzerland) (electrode InLab 730, measurement range of 0 µS/cm–1000 µS/cm) was used for investigations.

The temperatures of the exothermic effect of refractory castable pastes were determined based on the methodology developed by Alcoa. Temperature development, which results from the exothermic (EXO) reaction of the aluminate cement hydration using various fillers, was followed according to the methodology [47] using laboratory-designed equipment. Fresh mix paste (1.5 kg) was poured into the laminate mould (100 × 100 × 100 mm), then a thermocouple of type T was placed in the centre of the mould. The mould was compacted for 1 min on the vibrating table and placed in a steel box coated with a layer of expanded polystyrene (50 mm) from the inside. A computer recorded the temperature change every minute.

Observations of changes in the structure of refractory castable samples were carried out with the help of the PUNDIT 7 device (Proceq SA, Schwerzenbach, Switzerland), measuring the speed of propagation of the ultrasonic pulse in the samples after treatment at different temperatures. The non-destructive ultrasound pulse velocity test was chosen because it is possibly the most advanced method due to its clear physical basis, accuracy, and ease of use. This method is used to monitor the setting, hardening behaviour and development of the structure of cement paste and refractory castables [48]. The ultrasonic pulse velocity (UPV) method was applied using the ultrasonic pulse indicator PUNDIT 7 with the two 54-kHz standard cylindrical transducers (transmitter and receiver) to evaluate the structure development of the samples. Fresh pastes were set between two ultrasonic transducers operating at 10 pulses per second and a frequency of 54 kHz. The transducers were pressed against the samples at the two strictly opposite points. The value of UPV in the samples was tested after hardening, drying, and firing. Vaseline was used to ensure good contact. The UPV (V) was calculated from the following equation:

$$V = \frac{l}{\tau} \cdot 10^6 \quad (2)$$

where l represents the length of the tested mortar sample (distance between cylindrical heads), and τ is the time of pulse spread.

Observations of changes in the structure of refractory castable samples were carried out with the help of the same PUNDIT 7 device, measuring the speed of propagation of the ultrasonic pulse in the samples after treatment at different temperatures.

Fired at 1100 °C, sample structure analysis was conducted using a scanning electron microscope SEM EVO 50 EP (Carl Zeiss, SMTAG, Germany, resolution 1.5 nm).

The phase analysis of CSF was carried out by X-ray diffraction using the diffraction meter DRON-7 (Bourevestnik, JSC, Saint-Petersburg, Russia, Ni filter, Cu anode, anode emission current of 12 mA, anode operating voltage of 30 kV, goniometer apertures (0.5; 1.0; 1.5 mm)). The phase composition was identified using the reference data from the ASTM database.

The preparation of concrete samples and determination of their main physical and mechanical characteristics (compressive strength, density, and deformations) and the drying and firing of the refractory castable were conducted following EN 1927 [49].

The compressive strength of the refractory castable was measured after 3 days, 7 days, and 10 days of hardening, as well as after drying and firing at temperatures of 800 °C, 1000 °C, and 1100 °C. These tests were performed using an ALPHA3-3000S hydraulic press (FORM+TEST Seidner & Co. GmbH, Riedlingen, Germany) in compliance with the requirements of EN 12390-3:2019 [50].

3. Results

3.1. EC and pH

Coal-firing ash mainly shows acidic reactions [51]. This circumstance can affect the course of cement hydration; therefore, the effect of CSs on the electrical conductivity (EC) and pH of an aqueous and cement suspension was determined. The study shows that the effect of CSs on the electrical conductivity (EC) and pH of an aqueous solution is low–351 mS/cm and 5.6, respectively. The EC of water suspension of NS is higher than that of CSs and reaches 667 mS/cm, but the pH of water suspension is a lower 5.2. The pure cement suspension (K-0) displays at the start of measurement 2220 mS/cm EC value, which after 15–20 min reaches 2880 mS/cm EC value (Figure 7).

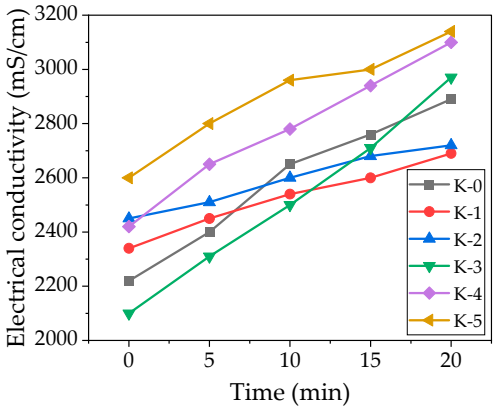


Figure 7. Changes in electrical conductivity (EC) of suspensions with the separate addition of CSs or NS, and with CSs and NS used together within 20 min.

In cement suspensions, the addition of CSs in the initial period contributes to an increase in the EC values compared to the pure cement suspension (K-1 and K-2). The EC values of the cement suspension with CSs are increased because CSs bring additional ions to the suspension, appearing from coal-firing products, such as alkali components. However, at higher CS content levels, the transition of ions into the suspension slows down, and the increase in EC is not very obvious. After 15–20 min, the EC values in pure cement suspension exceed the EC values of suspensions with the addition of CSs. The higher the CS content in the suspension, the lower the EC growth rate. It shows that higher amounts of CSs can retard the cement minerals dissolution process.

In cement suspensions, adding NS (K-3) in the initial period contributes to significantly lower EC values than with CSs and reaches 2100 mS/cm. However, after 10 min, the speed at which the EC values increase is the highest among tested suspensions. After 15–20 min, the EC values reach 2970 mS/cm and are higher than in the pure cement suspension. It shows that NS addition lessens the retardation of the cement minerals dissolution process. This research shows that NS increases cement suspension EC more effectively at the early hydration time than CS. In cement suspensions with the addition of both NS and CSs (K-4 with a lower CS amount and K-5 with a higher CS amount), the EC values of suspensions are higher than in suspensions with separately used CSs and NS at the start and finish of measurements. It means that using both CSs and NS in cement suspension does not retard cement hydration.

The study's data show that CSs reduce the growth rate of EC and pH in suspensions and possibly inhibit the transition of cement minerals into the suspension. NS starts to promote EC growth at a later period of hydration.

The pH values in the pure cement suspension within 20 min increased from 11.1 to 12.5 (Figure 8). When the pH values in suspensions decrease to a greater extent, the CS

content in the suspension is higher. The rate of pH growth also decreases with an increasing amount of CSs in the suspension, which can be explained by the low-acidic nature of CSs. For the same reason, the presence of NS decreases the pH value in suspension. When CSs and NS are used together in the cement suspension, the pH value is practically the same as in suspensions where CSs and NS were used separately.

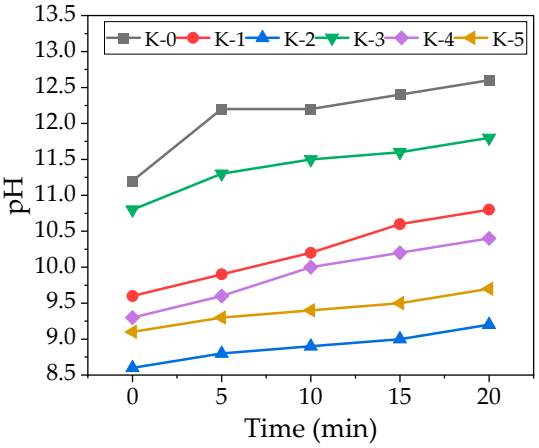


Figure 8. Changes in pH of suspensions with the separate addition of CSs or NS, and with CSs and NS used together within 20 min.

3.2. Spread

The studies conducted on the castable mix spread diameter showed that the presence of NS in the composition showed a slight decrease in spread compared to the control mix (Figure 9). An increase in the amount of CSs in the composition led to a decrease in the spread diameter from 15.5 cm to 10.5 cm, respectively, down by 32.3%. This result can be related to the uneven porous cenosphere surface. An amount of CSs exceeding 20% in the composition should be used with a higher water amount because the spread value of less than 11cm means the castable will have difficulties with mix laying. Completely different trends are observed when prewetted CSs are used in compositions. Prewetting of CSs increases spread value as follows: compared to using 10% of non-prewetted CSs, the value is up by 12%; compared to 15% of non-prewetted CSs, the value is up by 18.8%; compared to 20% of non-prewetted CSs, the value is up by 20.8%, and compared to 25% of non-prewetted CSs, the value is up by 22% (Figure 10). These results prove a positive influence of the prewetting of CSs. Prewetted CSs do not adsorb water. Water layers may appear around each CS particle, lubricating particles and increasing spread values.

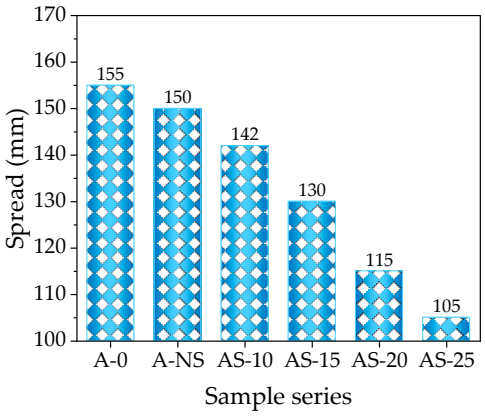


Figure 9. Spread of concrete mix with non-prewetted CSs.

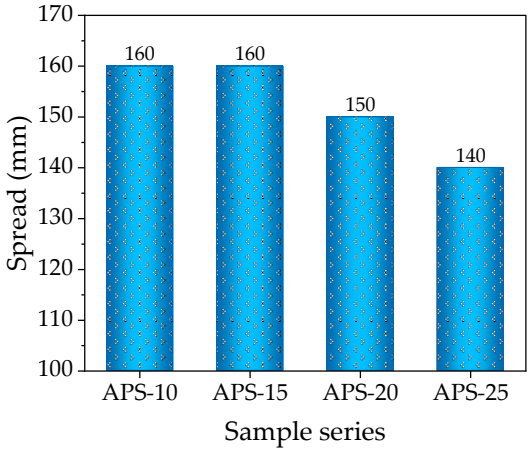


Figure 10. Spread of concrete mix with prewetted CSs.

3.3. UPV

The densification of castable sample paste structure during hydration is reflected in UPV tests [52]. The research on the densification of the structure of fresh refractory castable paste A-0, A-NS, AS-15, AS-25, APS-15, and APS-25 right after paste preparation during 24 h is presented in (Figure 11). Results show that in paste A-0, the induction period is about 4 h. In the ANS paste, the induction period is shorter–3 h. When CSs comprise a lower amount in composition (15%), the induction period decreases to 2 h, but with increased CSs to 25% in composition, the induction period extends to 6 h. The retardation of cement mineral dissolution can explain this prolongation of the induction period because of water decreasing in solution due to water absorption by CSs. The water amount is significant because with an increase in CS amount, water in the mix increases as part of the water necessary for cement hydration is adsorbed on the surface of CSs. With many voids and cavities, the surface of each CS can adsorb a significant amount of water and decrease free water to cement particles. This effect can decrease cement ion transition in the paste and retard hydration [53]. These findings are consistent with those reported in the investigation of the refractory castable pastes' EXO profiles and reflect the influence of the CS amount in a refractory castable paste. In the case of prewetted CSs, the induction period prolongs to 14 h for APS-15 and 15 h for APS-25. That means less water can be used to participate in hydration because mixing water was used less for these compositions. Another reason is the water, saturated inside of CS, which does not participate at the start of the hydration process but requires additional heat from the hydration of cement to increase the paste temperature [44,54].

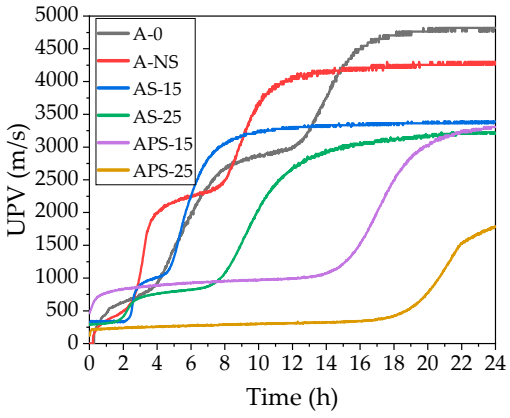


Figure 11. The hydration process in the concrete mix, depending on the amount of non-prewetted and prewetted CSs in the composition.

A sharp increase in the UPV during the massive precipitation of cement mineral hydrates occurs during the next 5–10 h for A-0, A-NS, AS-15, and AS-25 pastes. The addition of NS, compared to plain castable paste A-0, increases the speed of structure formation of the paste by almost two times. After 5 h of hydration in this paste, UV reaches 2000 m/s, whereas in A-0 paste, UPV is only about 1000 m/s. In the AS-15 and AS-25 pastes, a sharp increase in the UPV is observed after 6.6 h and 9 h, and values reach 3100 m/s and 2840 m/s.

When prewetted CSs were used, the structure densification is prolonged and is more visible. In the case of prewetted CSs, the induction period is significantly prolonged. In this case, mixing water was used less for these compositions. Another reason is the water, saturated inside of CSs, which does not participate at the start of the hydration process but requires additional heat from the hydration of cement to increase the paste temperature. A sharp increase in the UPV is observed after 20 h and 21 h for APS-15 and APS-25.

As we can see, in pastes A-0 and A-NS, the next step (third) is growth in UPV observed after 13 h and 8 h. For compositions containing CSs, the structure development takes place in two steps. After 24 h of curing, the highest UPV values, 4800 m/s, have been reached in paste A-0, the lowest in APS-25–2500 m/s. This difference in the hydration steps can be related to different water releases in the paste. Free water in the system, not captured in the CSs, increases the speed of hydration, but soaking it in CS water can help it to participate in hydration later. The final densification after 24 h of hydration reflects this tendency. Prolonged densification with prewetted CSs reflects a prolonged hydration process because of retarded water penetration to the cement particle.

3.4. EXO Profile

To evaluate whether the heat emitted during cement hydration affects EXO, fresh cement pastes were tested (Figure 12). Studies of the temperature and time of the EXO maximum of the pastes showed that in the control composition A-0, the EXO maximum is achieved after 17 h, and the temperature of the EXO effect reaches 46.7 °C. When NS is added to the composition, the EXO effect appears after 13.5 h, and the temperature of the EXO effect reaches 47.2 °C. As pointed out in research [25], NS brings forward the time of the EXO maximum by 20%.

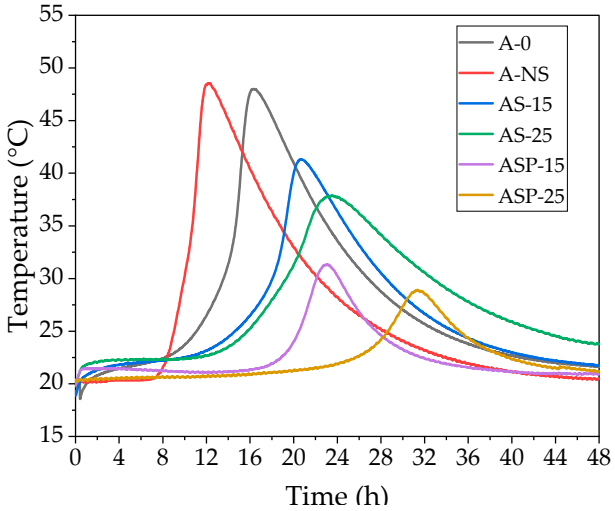


Figure 12. The EXO time and temperature in concrete mix depending on the amount of CSs in the composition.

Lower pH of NS and CSs leads to visible prolongation of the cement minerals dissolution process, reflected in an increase of the EXO time. The test results showed that with the

replacement of GCM aggregate to CSs up to 15% and 25% in the paste, the EXO maximum time was prolonged to 20 h and 23.8 h.

Possibly, such an effect can be explained by the surface of a CS itself–pores and voids, which absorb water, and retard water entrance to cement minerals. Additionally, limiting the amount of water reaching the cement can retard the hydration of cement [55]. EXO maximum temperature for this composition decreases to 42 °C and 37.5 °C. However, the temperature of the EXO effect decreases not significantly by 10.1–20.2%, which may be due to the pozzolanic activity of the amorphous phase of CSs, which reacts with cement hydration products [56] and lowers hydration temperature. Higher amounts of CSs decrease the temperature, possibly due to the lower amount of cement minerals that can react with pozzolana. NS, equally, has pozzolanic activity and participates in the cement hydration process [57].

The same was observed in [58,59] compared with pure cement; the EXO maximum time for compositions with alumosilicate spheres' ash was prolonged. That is related to alumosilicate spheres' ash having low acidic pH and a high specific surface area. At the same moment, possibly due to their lower pH, CSs can have a slightly lower intensity of hydration and, in such a way, decrease the EXO maximum temperature.

When the amount of prewetted CSs increased to 15% and 25% in the composition, the EXO maximum time was prolonged, up to 21 h and up to 29.2 h, and the EXO maximum temperature decreased to 32 °C and 28 °C. Prewetted CSs decrease the EXO maximum temperature by 31.4–40.4%, and EXO maximum prolongation is up to 23.5% and 73%, compared to A-0 composition.

Based on the method [60], it is possible to evaluate the effect of the non-prewetted and prewetted CS additive according to the following parameters: a decrease in the temperature of the EXO effect (T), an increase in the time of the EXO effect (H), change (decrease or increase) in the rate of temperature rise compared to a reference sample, and EXO reaction speed in °C/min for all tested compositions (Table 4). According to the results in Table 4, the rate of temperature with the addition of NS increased from 0.057 °C/min to 0.113 °C/min. With the addition of CSs, the rate of temperature rise decreases. The increase in non-prewetted CSs has changed from 0.041 °C/min to 0.028 °C/min. The rate of temperature rises with an increasing amount of prewetted CSs, changing from 0.020 °C/min to 0.011 °C/min.

Table 4. The influence of non-prewetted and prewetted CSs on various hydration parameters of compositions.

	Decrease in T, %	Change in H, %	Change in EXO Reaction Speed, °C/min
A-0	–	–	0.057
A-NS	Increase 1.1	Decrease 12.5	0.113
AS-15	10.1	Increase 15	0.041
AS-25	20.2	Increase 28.6	0.028
APS-15	31.4	Increase 23.5	0.020
APS-25	40.4	Increase 73	0.011

The EXO reaction speed for prewetted CSs decreased by 48.7% and 39.3% compared to non- prewetted CSs. Based on the results in Table 4, replacing 25% of milled chamotte with prewetted CSs can be marginal for refractory castable mixture because of significantly prolonged hydration time, which complicates the application technology of such castables.

The results of ultrasound studies in samples after 7 days of hardening, drying, and firing are presented in Figure 13. After the first day, the highest UPV values are recorded in the A-0 composition. NS addition reduces UPV values by up to 10.6%. An increase

in the amount of CSs in the composition contributes to a significant decrease in UPV values–by up to 25% compared to A-NS samples. Perhaps the physical properties (big surface area, presence of pores on the surface) of the CSs themselves affect the speed of UPV in the samples (Figure 5). After the third day, UPV values increase in all compositions, but mainly in the A-NS composition. It seems that happens because of the pozzolanic properties of NS [61]. After 7 days of curing, UPV values mainly increased in the samples A-NS, APS-15, and APS-25–by up to 13.9%, 20.54%, and 23.53%. This result shows that the pozzolanic properties of NS primarily support the hydration process in the samples with prewetted CSs. It is possible that water adsorbed into CSs releases and participates in the hydration process.

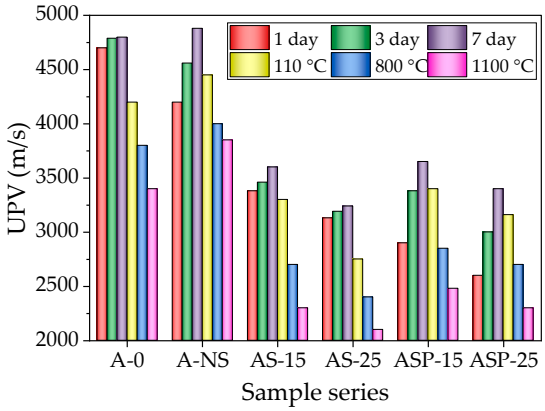


Figure 13. UPV in the castable samples, depending on the amount of CSs and their pretreatment in the composition.

The drying process significantly influences the structure of samples and decreases UPV values. However, the reduction of UPV values occurs differently in the samples. Mostly, UPV values decrease in the A-0 and ANS-25 samples–by up to 12.8% and 15.1%, and in the A-NS and ANS-15 samples–by up to 9.1% and 9.7%. Prewetting of CSs decreases the structure deterioration. UPV values decrease in samples APS-15 and APS-25 by up to 6.7% and 7.05%. Such results suggest that during the more extended curing and further drying process, the samples with prewetted CSs create new hydration products, which involve more water, and the structure becomes denser and less damaged by cracks during water evaporation [25].

As the processing temperature increases, the UPV values drop due to the destruction processes (water evaporations, decomposition of hydrates, the appearance of new ones) occurring in the specimens. The results of ultrasound tests in samples after firing at 800 °C and 1100 temperatures show that the greatest UPV drops were in the ANS-15 and ANS-25 samples–by up to 30.3% and 25.6%. The lowest drop in UPV values is observed in samples with prewetted CSs, APS-15 and APS-25, by up to 23% and 22.4%. It is known that adding CSs to the composition generally decreases UPV values. UIG values more significantly drop due to the porous structure of CSs after firing at 800 °C and 1100 temperatures [62].

The lowest drop is observed in samples A-0 and A-NS, 19.18% and 13.5%. As can be concluded, prewetting decreases structure destruction compared with non-prewetted CSs. It is known adding CSs to the composition generally decreases UPV values [24]. UIG values more significantly drop due to the porous structure of CSs after firing at 800 °C and 1100 temperatures. The lowest drop in UPV in samples A-NS can be related to new dense phase creation in the structure of the sample during firing [25].

Studies of the density of the samples (Figure 14) showed that NS addition does not significantly affect the density of samples, but an increase in the amount of CSs in the

composition results in a notable decrease in the density of the samples. After curing for 7 days, the difference in density of samples A-0, A-NS, and ANS-15, ANS-25 is as follows: 2010 kg/m^3, 2025 kg/m^3, 1639 kg/m^3, and 1421 kg/m^3. Adding CSs decreased density by up to 29.82% compared to the A-NS sample density. In the samples with prewetted CSs, the decrease in density is up to 21.5%. After drying, this difference for ANS-15, ANS-25 samples reached 30.1%, but samples with prewetted CSs reached 28.7%. While firing at a temperature of 800 °C, the density of the samples further decreases. With further firing at a temperature of 1100 °C, a slight increase in the density of the samples A-0 and A-NS is observed due to sintering processes. In the samples with CSs, the density after firing decreased a little. It can be observed that the density of samples with prewetted CSs is higher than that of samples of the same composition without prewetted CS. Generally, it can be concluded that adding CSs reduces the density of the samples over the entire temperature range.

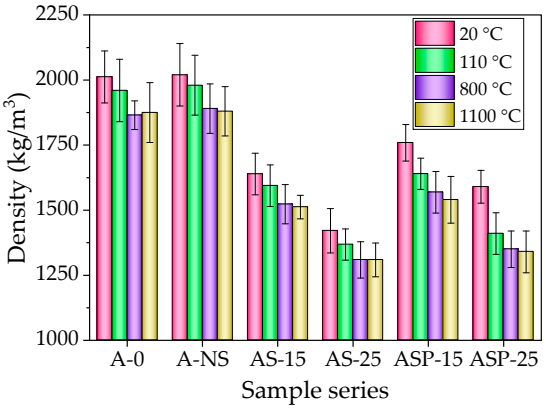


Figure 14. The density of castable samples, depending on the amount of CSs and their pretreatment in the composition.

After hardening, compressive strength tests of samples (Figure 15) showed that adding NS in the A-NS composition increases compressive strength by just 2%. Increasing the amount of CSs to 15% and 25% in the composition reduces the strength by 56% and 76.5%, compared to the A-NS sample. In the case of prewetted CSs, the compressive strength is reduced by 60% and 77% compared to the A-NS sample.

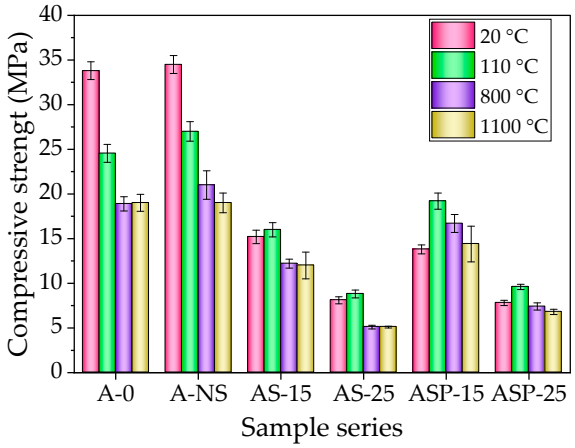


Figure 15. Compressive strength of castable samples, depending on the amount of CSs and their pretreatment in the composition.

After drying, the strength of the samples from compositions A-0 and A-NS decreases. However, the compressive strength of A-NS samples is 13% higher than A-0 samples. This

increase in strength can be explained by the influence of new formations in samples, such as stratlingite (C_2ASH_8). The study [63] explored that in the presence of siliceous components, such as microsilica or NS, the formation of stratlingite in dried cement samples was observed. During drying, hydration reactions are accelerated in the presence of NS, as the primary hydration product C_2AH_8 interacts with siliceous components to form stratlingite, contributing to improved mechanical properties. At the same time, in composition, less C_3AH_6 is formed, leading to a decrease in porosity and, at the same time, an increase in strength [64].

In samples ANS-15 and ANS-25, compared to compressive strength values after curing, the strength after drying increases by up to 22.6% and 8%, but in the samples with prewetted CSs (APS-15, APS-25), the strength increases by up to 28.4% and 22%. This result suggests that prewetted CSs, due to additional water provided in the system during drying, can increase the additional formation of mineral C_2AH_8 and, as a result, new minerals, such as stratlingite, are created. The mineral stratlingite is responsible for increasing the compressive strength of samples. Such observation is supported in research [25].

Following heat treatment at 800 °C, the strength in compositions A-0 and A-NS decreases by 24% and 22% compared to the strength after drying. In samples ANS-15 and ANS-25, the strength decreased by 31.1% and 56.9%; in samples APS-15 and APS-25, the strength decreased by 27.5% and 47% compared to the strength after drying. Further firing at 1100 °C reduces the strength in samples A-0 by up to 15.3%, compared to firing at 800 °C. In the A-NS sample, the strength reduction reached 9%. In samples ANS-15 and ANS-25, the strength mainly decreases by 22.3% and 24.7%, and in the APS-15 and APS-25 samples, the observed decrease was lower–reducing by only 12.8% and 13.4%.

This result represents the positive effect of prewetting. Prewetted CSs influence the strength maintained after firing at high temperatures. New stratlingite structures created during the dehydration process may form spatial contact structures (zones) in the castable matrix and contribute to the development of strength characteristics and the reduction of internal stresses in the castable during firing. Furthermore, prewetted CSs promote the early formation of anorthite after firing.

The calculated ratio of the strength of samples A-0, A-NS, ANS-15, ANS-25, and APS-15 and APS-25 to their density after firing at a temperature of 1100 °C (as follows: 0.86; 1.01; 0.66; 0.31 and 0.86; 0.5) shows that the most advantageous in terms of this ratio are compositions A-NS and APS-15.

An XRD study was performed to explain the different compressive strengths in samples with CSs after drying. These differences are reflected in mineral formation during drying when the NS amorphous phase can react with cement minerals (Figure 16) [57].

XRD has shown that during exposure at a temperature of 110 °C in the sample AM-0, the crystalline hydrate CAH_{10} ($CaO{\cdot}Al_2O_3{\cdot}10H_2O$) and C_2AH_8 ($2CaO{\cdot}Al_2O_3{\cdot}8H_2O$) dominates from the new formations, but in the sample with NS (AM-NS) together with CAH_{10} and C_2AH_8, stratlingite crystallises more actively. During drying, hydration reactions proceed more intensively in samples with NS, in which C_2AH_8 reacts with NS and the mineral stratlingite is formed. AH_3 ($Al_2O_3{\cdot}3H_2O$) and C_3AH_6 ($3CaO{\cdot}Al_2O_3{\cdot}6H_2O$) crystal hydrates were identified in samples without NS. However, AH_3 predominates in samples with NS addition, while denser C_3AH_6 predominates in control samples. The structure created during the drying process may have represented the mineral formation during burning, which could explain the notable variation in the samples' strength properties. XRD analysis was performed on the control sample and the sample with NS addition to clarify this assumption. Samples were burned at 900 °C, 1000 °C, and 1100 °C. (Figure 17). According to research [65], the formation of the mineral stratlingite and the change in the ratio of the minerals C_3AH_6 and AH_3 in the cement matrix is a possible reason for the

increase in the strength of castable samples with NS addition, since the resulting stratlingite, during further firing, crystallises into the mineral anorthite. The mineral C_3AH_6 during the dehydration process is converted into the mineral $C_{12}A_7$ ($12CaO{\cdot}7Al_2O_3$), which, during burning, reacts with the NS and forms the mineral gehlenite [66].

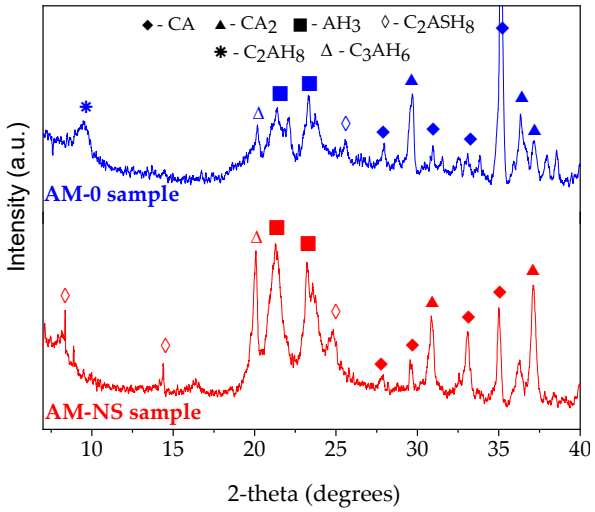
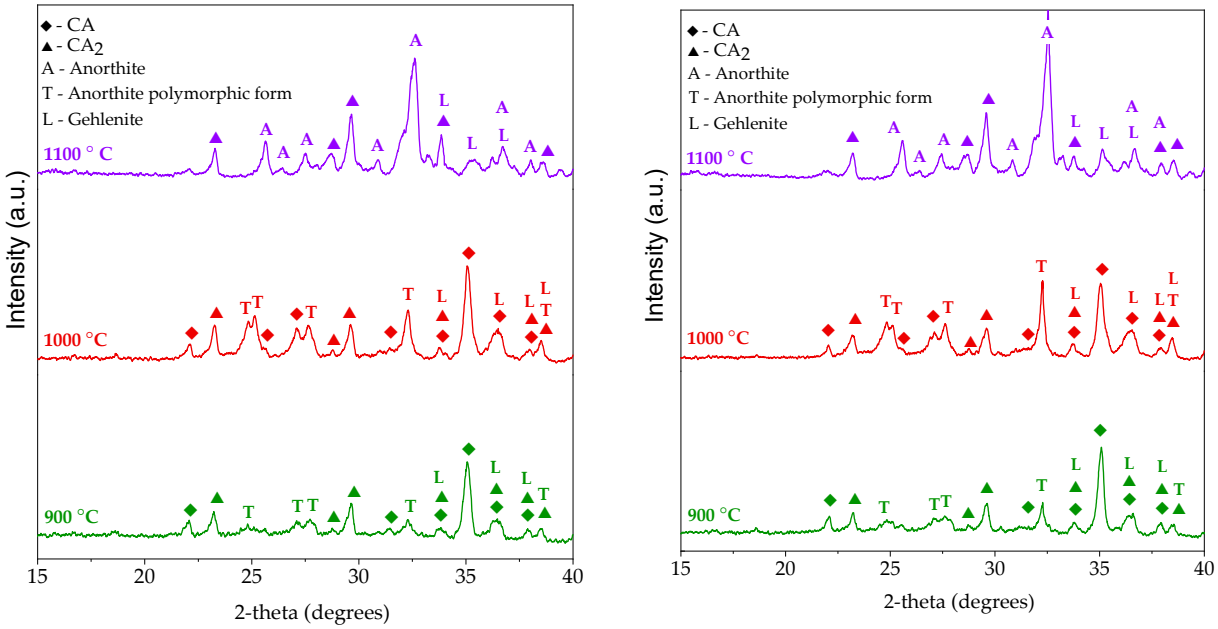


Figure 16. X-ray diffraction patterns of samples of compositions AM-0 and AM-NS after drying at a temperature of 100 °C.



(**a**) (**b**)

Figure 17. X-ray diffraction patterns of the compositions (**a**) AM-0 and (**b**) AM-S after firing at temperatures 900 °C, 1000 °C, and 1100 °C.

After firing the samples at a temperature of 900 °C, which was carried out to detect the onset of crystallisation of new formations in the cement stone, the minerals CA, CA_2 $Ca_2Al(AlSi)O_7$ (gehlenite) were found in the AM-0 sample. In the sample with NS together with CA, CA_2, $Ca_2Al(AlSi)O_7$, the onset of the formation of polymorphic form of anorthite ($CaO{\cdot}2Al_2O_3{\cdot}2SiO_2$) was recorded.

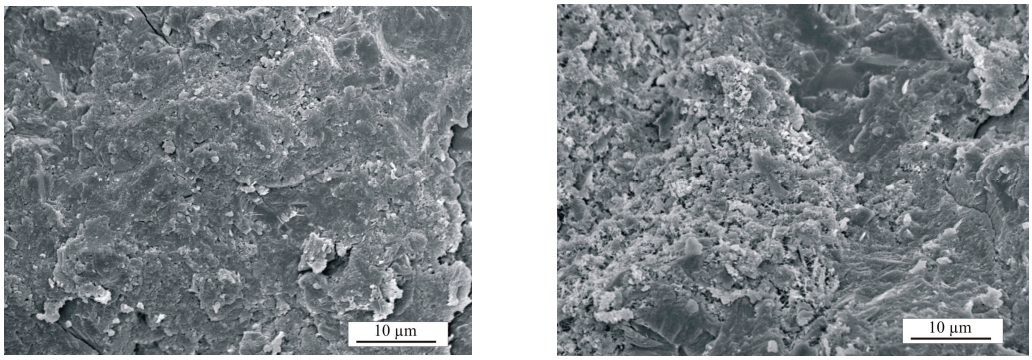
After firing at 1000 °C, the CA minerals and gehlenite crystallise more actively in the control sample. The polymorphic form of anorthite crystallises more actively in samples

with NS. This mineral is more active because stratlingite participates in its crystallisation, and Si is more extensively involved in the synthesis reactions than other processes. This indicates an increase in the binding of the silicate component in these compositions [67] and proves that the polymorphic form of anorthite is a precursor to the early formation of stable anorthite. Besides this, the density of the polymorphic form of anorthite is 2.7 g/cm^3, but anorthite density is 2.78 g/cm^3 [68,69]. This difference shows that anorthite can create crystals with higher volume and be more resistant to thermal stress [70,71].

In both samples of AM-0 and MA-NS compositions fired at 1100 °C, CA was not identified since it reacts with the silicate components of the cement stone and participates in the formation of gehlenite and anorthite ($CaAl_2Si_2O_8$). The polymorphic form of anorthite was also not identified, but the more intense crystallisation of anorthite in the A-NS sample substantiates the assumption that it transforms into anorthite. It can be assumed that the control sample promoted more active calcium binding (formation of gehlenite), and the sample with NS promoted more active binding of the silicate component with the formation of anorthite, which is more refractoriness, less dense than gehlenite [71–73].

The results obtained indicate that during the drying process, the formed stratlingite is less susceptible to transformations during further heat treatment than the framework of C_3AH_6 and AH_3 crystal hydrates, and after firing it promotes the formation of anorthite, which has a higher hardness than the mineral gehlenite. That is possibly the reason for the increase in the strength of concrete samples of compositions with NS.

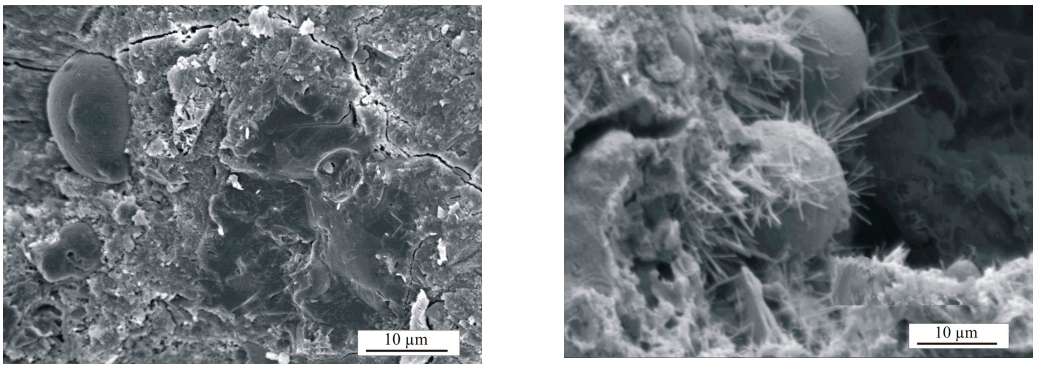
Conducted SEM studies after the drying procedure showed that the microstructure of cement matrix samples AM-0 and samples with non-prewetted and prewetted CSs differ. In the microstructure of the cement matrix AM-0 (Figure 18a), large aggregates of the mineral CA dominate. Hydration products are not visible. In the sample (AM-NS), the view is slightly different. The structure presents many hydrates accumulating between coarse cement particles (Figure 18b).



(**a**) (**b**)

Figure 18. Macrostructure of a cement matrix sample (**a**) AM-0 and (**b**) AM-NS.

The structure of samples AS-20 and APS-20 is presented in Figure 19. It is seen that no new structures appeared around the CS particle in the AS-20 sample. CSs are just imbedded in the cement matrix. In the case of prewetted CSs, the view is different. There are a lot of different shapes of hydrates around the CS, and needle-shaped hydrates cover the surface of the CS. The needle-shaped hydrates can belong to CAH_{10} or crystals of AH_3, and the small plate-shaped hydrates in the matrix can belong to poorly crystallised C_2AH_8 and stratlingite. Because samples were dried at 100 °C temperature, it is more likely that CAH_{10} are destroyed during dehydration, and there may be AH_3 hydrates.



(**a**) (**b**)

Figure 19. Macrostructure of a cement matrix sample (**a**) AS-20 and (**b**) APS-20.

Figure 20 presents a more detailed view of the APS-20 sample matrix. It is observed that agglomerates with small plate-shaped hydrates and AH_3 (size about 10 µm) are positioned in the intermediate spaces. The size of the small plate-shaped hydrates is at least 10–20 times smaller than AH_3. Studies have confirmed the presence of such crystal hydrates [25]. This structure of samples confirms compressive strength results. Studies have also shown that during the formation of stratlingite, less C_3AH_6 is formed, which leads to a decrease in porosity and, at the same time, an increase in compressive strength [64]. New stratlingite structures during dehydration may form spatial contact structures (zones) in the concrete matrix and contribute to the development of strength characteristics and the reduction of internal stresses in concrete during firing. During drying, hydration–dehydration reactions proceed more intensively in samples with microsilica and NS because C_2AH_8 reacts with NS (or microsilica) and the mineral stratlingite is formed [25].

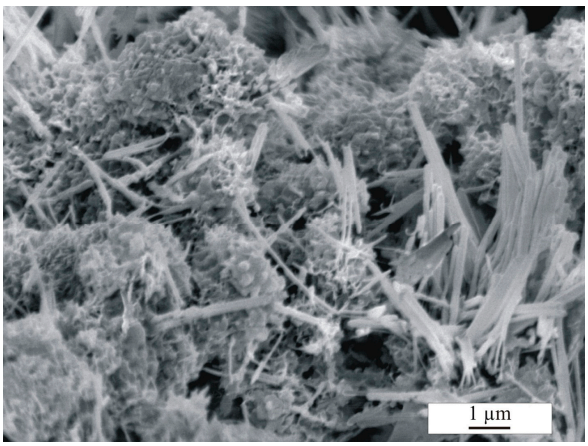


Figure 20. Microstructure of a cement matrix sample APS-20.

Shrinkage research of all composition samples after firing at temperatures of 800 °C and 1100 °C has shown that adding NS increases the shrinkage of samples, compared to the A-0 sample (Figure 21). An increase in the amount of CSs (non-treated and prewetted) proportional to the amount in the castable composition reduces the shrinkage of samples after firing at pointed temperatures. In compositions ANS-15, ANS-25, APS-15, and APS-25, after firing at temperatures of 800 °C, the highest shrinkage is observed for AS-15 samples (0.2%) and the lowest for ASP-25 samples (0.1%). After firing at temperatures of 1100 °C, the highest shrinkage is observed for AS-15 samples (0.25%) and the lowest for ASP-25 samples (0.1%). It can be concluded that after firing at a temperature of 1100 °C, non-pretreated CS amounts (amounts of 15% and 25%) reduce shrinkage by 34.2% and 57%, compared to A-NS composition samples. Compared to A-NS composition samples, prewetted CSs in

compositions APS-15 and APS-25 reduced shrinkage by 38% and more than three times. Mineral mullite, which is detected in the CSs, also positively affects the strength and shrinkage of the samples [4]. Prewetting increases compressive strength while decreasing shrinkage. Along with low density and shrinkage, samples with CSs demonstrate relatively high compressive strength values. It can be noted that the ultrasound results correlate well with the results of density, strength and shrinkage.

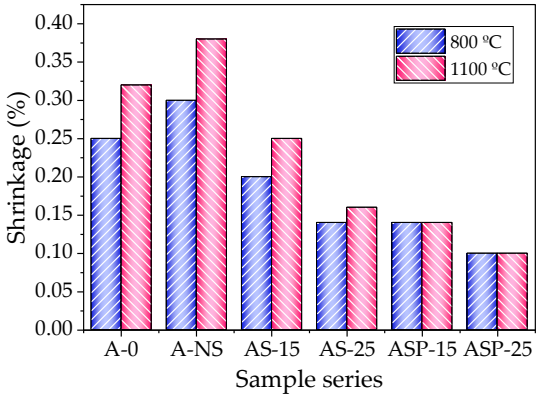


Figure 21. Shrinkage of castable samples, depending on the amount of CSs and their pretreatment in the composition.

Finally, a hypothesis of the whole mechanism of the positive effect of both nano silica and prewetted cenospheres' interaction during the drying process can be shortly described. Two components exist, such as a cenosphere capable of retaining water for a longer period and active nano silica, capable of interacting with cement minerals during hydration. The increase in strength can be explained by the influence of new formations between cement minerals and nano silica, such as stratlingite (C_2ASH_8). During drying, the captured in cenospheres' water can rapidly release and enter the cement matrix, which stimulates the hydration process. Unreacted cement minerals can be hydrated. During drying, hydration reactions are accelerated in the presence of nano silica, as the primary hydration product C_2AH_8 interacts with siliceous components to form stratlingite, contributing to improved mechanical properties. An additional possible reason to increase the compressive strength of concrete after drying is CA_2 hydration, which is strongly increased when the treatment temperature reaches 40 °C or more. Mineral mullite, which is detected in the CSs, also positively affects the strength and shrinkage of the concrete. Prewetting due to new mineral phasis increases compressive strength and the stability of the frame without affecting the increase in shrinkage.

4. Conclusions

1. Test results show that the aqueous suspension of CSs and NS has an EC of 351 mS/cm and 667 mS/cm, and the pH of water suspension is 5.6 and 5.2. Therefore, in cement suspensions, an increase in the addition of CSs contributes to an increase in the initial EC values and a decrease in pH. On the contrary, NS in cement suspensions decreases the initial EC values but does not significantly change pH. CSs reduce the growth rate of EC and pH in suspensions and possibly inhibit the transition of cement minerals into the suspension. The presence of NS starts to promote cement dissolution and EC growing at the later hydration period.
2. Due to the physical characteristics of CSs (porous surface), increasing the CS content in the composition up to 15% and up to 25% leads to deterioration of rheological properties, a decrease in the spread diameter of the castable mix by up to 14.5% and up to 31%. Due to water layers created on the CSs' surface, the prewetting of

CSs significantly improves the rheological properties of the castable mix. When the amount of prewetted CSs is 15% in the mix, the spread diameter increases by up to 5%, compared to the reference mix without CSs. A higher amount of CSs (up to 25%) leads to a decrease in the spread diameter of the castable mix by up to 7.9%.

3. The tested electrical conductivity and pH of CSs and NS in suspensions influence the EXO profile and early structure formation of castable mixtures. An increased amount of non-prewetted and prewetted CSs to 15% and 25% prolongs the structure formation period in the mixes up to 1.9 and 3 times, prolongs the time of EXO maximum by up to 15% and 28.6%, and 23.5% and 73%, and reduces the EXO effect temperature by up to 10.1% and 20.2%, and by 31.4% and 40.4%, compared to the reference mix. In the case of non-prewetted CSs, it happens due to the porous nature of CSs, which adsorb the mixing water, resulting in the retardation of the dissolution process of cement minerals. In the case of prewetted CSs, more significant retardation is caused by water slowly diverging from the CSs to the environment. Using an amount of prewetted CSs of 25% contributes to the prolongation of hydration time. That is why applying such an amount of CSs in refractory castable technology must be carefully conducted.
4. Proportionally to the increase in the amount of non-prewetted and prewetted CSs in the composition, the density of the samples decreases by 30.3% and 28.5% after firing at a temperature of 1100 °C. Contrary to the control composition, the amount of CSs varied from 15% to 25%, increasing compressive strength by 5.3% and 8.6% (non-prewetted CSs) and 39.2% and 20.5% (prewetted CSs) after drying. After firing at 800 °C temperature, the same amounts of CSs in the composition decrease compressive strength by 41.9% and 75.7% (non-prewetted CS), and 20.3% and 64.5% in the case of prewetted CSs. After firing at 1100 °C, the mentioned amounts of CSs decreased compressive strength by 36.8% and 73.16% (non-prewetted CS) and by 24.0% and 64.2% in prewetted CS, compared to the control sample.
5. During the drying process, the formed stratlingite in the composition with NS is responsible for the increase in mechanical properties; the structure is less susceptible to transformations during further heat treatment and, after firing, it promotes the early formation of anorthite.
6. According to the parameters of the ratio of the strength of samples to their density, the amount of CSs of 15% in the composition is optimal. The shrinkage of the refractory castable samples with CSs decreased after firing at 800 °C from 0.3% (control sample) to 0.14% in the case of non-prewetted CSs and to 0.1% in the case of prewetted CSs. After firing at 1100 °C, the shrinkage of samples decreased from 0.34% (control sample) to 0.16% in the case of non-prewetted CSs and to 0.1% in the case of prewetted CSs. The highest CS amount allows for a significant reduction in shrinkage. The porous structures formed in samples containing 15% and 25% CSs effectively dissipate stresses generated during firing, significantly mitigating shrinkage and enhancing dimensional stability.

Author Contributions: Conceptualization, I.P. and J.P.; methodology, J.P.; validation, J.P.; formal analysis, I.P.; investigation, I.P. and J.P.; resources, J.P.; data curation, I.P.; writing—original draft preparation, I.P. and J.P.; writing—review and editing, I.P. and J.P.; visualisation, J.P.; supervision, I.P. All authors have read and agreed to the published version of the manuscript.

Funding: This research received no external funding.

Data Availability Statement: The raw data supporting the conclusions of this article will be made available by the authors upon request.

Conflicts of Interest: The authors declare no conflicts of interest.

References

1. Lu, J.; Zhang, Z.; Li, Y.; Liu, Z. Effect of Alumina Source on the Densification, Phase Evolution, and Strengthening of Sintered Mullite-Based Ceramics from Milled Coal Fly Ash. *Constr. Build. Mater.* **2019**, *229*, 116851. [CrossRef]
2. Yan, S.; Ren, X.; Wang, W.; He, C.; Xing, P. Preparation of Eco-Friendly Porous Ceramic with Low Thermal Conductivity by High-Temperature Treatment of Foamed Solid Waste Based Geopolymer with Cenospheres. *Constr. Build. Mater.* **2023**, *398*, 131190. [CrossRef]
3. Wang, C.; Liu, J.; Du, H.; Guo, A. Effect of Fly Ash Cenospheres on the Microstructure and Properties of Silica-Based Composites. *Ceram. Int.* **2012**, *38*, 4395–4400. [CrossRef]
4. Agrawal, U.S.; Wanjari, S.P. Physiochemical and Engineering Characteristics of Cenosphere and Its Application as a Lightweight Construction Material—A Review. *Mater. Today Proc.* **2017**, *4*, 9797–9802. [CrossRef]
5. Ranjbar, N.; Kuenzel, C. Cenospheres: A Review. *Fuel* **2017**, *207*, 1–12. [CrossRef]
6. Zyrkowski, M.; Neto, R.C.; Santos, L.F.; Witkowski, K. Characterization of Fly-Ash Cenospheres from Coal-Fired Power Plant Unit. *Fuel* **2016**, *174*, 49–53. [CrossRef]
7. Lv, L.; Zhang, X.; Šavija, B.; Zhang, M.; Han, K.; Zhang, H.; Pei, C.; Zhu, J.; Xing, F. Self-Healing of Cementitious Materials Using Sustainable Cenosphere-Based Manufactured Aggregate. *Constr. Build. Mater.* **2024**, *419*, 135361. [CrossRef]
8. Salim, M.U.; Danish, A.; Torres, A.S.; Moro, C. Environmental Assessment of Cenosphere and GGBFS-Based Geopolymers: A Path to Greener Construction Materials. *Environ. Impact Assess. Rev.* **2025**, *110*, 107711. [CrossRef]
9. Jaworek, A.; Sobczyk, A.T.; Czech, T.; Marchewicz, A.; Krupa, A. Recovery of Cenospheres from Solid Waste Produced by Coal-Fired Power Plants. *Clean. Waste Syst.* **2023**, *6*, 100109. [CrossRef]
10. Patel, S.K.; Majhi, R.K.; Satpathy, H.P.; Nayak, A.N. Durability and Microstructural Properties of Lightweight Concrete Manufactured with Fly Ash Cenosphere and Sintered Fly Ash Aggregate. *Constr. Build. Mater.* **2019**, *226*, 579–590. [CrossRef]
11. Leong, G.W.; Mo, K.H.; Ibrahim, Z.; Radwan, M.K.H.; Ling, T.C.; Sinoh, S.S. Lightweight Cementitious Composites Incorporating Fly Ash Cenospheres and Perlite Microspheres. *Constr. Build. Mater.* **2023**, *404*, 133226. [CrossRef]
12. Rajesh, K.N.; Teena, J.; Raju, P.M. A Review on Performance of Cenosphere Utilization in Concrete. *Mater. Today Proc.* **2022**, *62*, 5567–5570. [CrossRef]
13. Danish, A.; Mosaberpanah, M.A.; Tuladhar, R.; Salim, M.U.; Yaqub, M.A.; Ahmad, N. Effect of Cenospheres on the Engineering Properties of Lightweight Cementitious Composites: A Comprehensive Review. *J. Build. Eng.* **2022**, *49*, 104016. [CrossRef]
14. Wu, Y.; Wang, J.Y.; Monteiro, P.J.M.; Zhang, M.H. Development of Ultra-Lightweight Cement Composites with Low Thermal Conductivity and High Specific Strength for Energy Efficient Buildings. *Constr. Build. Mater.* **2015**, *87*, 100–112. [CrossRef]
15. Agrawal, U.S.; Wanjari, S.P. Light-Weight and High Thermal Insulation Building Material; a Comparative Study between Cenosphere & Fly Ash. *Mater. Today Proc.* **2023**. [CrossRef]
16. Zhang, H.; Ma, W.; Gao, F.; Ge, Z.; Yang, M.; Fang, H.; Šavija, B. Rheology, Shrinkage, Mechanical Properties and Microstructure of Ultra-Light-Weight Concrete with Fly Ash Cenospheres. *J. Build. Eng.* **2024**, *98*, 111258. [CrossRef]
17. Kavinkumar, V.; Priya, A.K.; Praneeth, R. Strength of Light Weight Concrete Containing Fly Ash Cenosphere. *Mater. Today Proc.* **2023**. [CrossRef]
18. Huang, Z.; Liew, J.Y.R.; Li, W. Evaluation of Compressive Behavior of Ultra-Lightweight Cement Composite after Elevated Temperature Exposure. *Constr. Build. Mater.* **2017**, *148*, 579–589. [CrossRef]
19. Yadav, V.K.; Yadav, K.K.; Tirth, V.; Jangid, A.; Gnanamoorthy, G.; Choudhary, N.; Islam, S.; Gupta, N.; Son, C.T.; Jeon, B.H. Recent Advances in Methods for Recovery of Cenospheres from Fly Ash and Their Emerging Applications in Ceramics, Composites, Polymers and Environmental Cleanup. *Crystals* **2021**, *11*, 1067. [CrossRef]
20. Mondal, D.P.; Das, S.; Ramakrishnan, N.; Bhasker, K.U. Cenosphere Filled Aluminum Syntactic Foam Made through Stir-Casting Technique. *Compos. Part A Appl. Sci. Manuf.* **2009**, *40*, 279–288. [CrossRef]
21. Brooks, A.L.; Shen, Z.; Zhou, H. Development of a High-Temperature Inorganic Synthetic Foam with Recycled Fly-Ash Cenospheres for Thermal Insulation Brick Manufacturing. *J. Clean. Prod.* **2020**, *246*, 118748. [CrossRef]
22. Rani, R.; Jain, M.K. Physiochemical and Engineering Characteristics of Fly Ash and Its Application in Various Field—A Review. *J. Biodivers. Environ. Sci.* **2015**, *6*, 161–174.
23. Sun, K.; Wang, L.; Su, H.; Geng, J.; Zhang, Q.; Meng, B.; Wei, Z.; Wu, G. Damping Properties and Mechanism of Aluminum Matrix Composites Reinforced with Glass Cenospheres. *Trans. Nonferrous Met. Soc. China* **2024**, *34*, 2743–2755. [CrossRef]
24. Pundienė, I.; Korjakins, A.; Pranckevičienė, J.; Kligys, M. Effect of Silicon Carbide Aggregate, Prepared by Different Methods, on the Properties of Refractory Concrete with Cenospheres. *Ceram. Int.* **2018**, *44*, 15944–15953. [CrossRef]
25. Pundienė, I.; Pranckevičienė, J. The Synergistic Effect of Adding a Blend of Deflocculants and Microsilica on the Properties of High Temperature Resistant Lightweight Concrete with Cenospheres. *Constr. Build. Mater.* **2020**, *230*, 116961. [CrossRef]
26. Danish, A.; Mosaberpanah, M.A. Formation Mechanism and Applications of Cenospheres: A Review. *J. Mater. Sci.* **2020**, *55*, 4539–4557. [CrossRef]

27. Ngu, L.N.; Wu, H.; Zhang, D.K. Characterization of Ash Cenospheres in Fly Ash from Australian Power Stations. *Energy Fuels* **2007**, *21*, 3437–3445. [CrossRef]
28. Sen, S. *Physical Properties of Cenosphere*; National Institute of Technology: Rourkela, India, 2014.
29. Urunkar, Y.; Pandit, A.; Bhargava, P.; Joshi, J.; Mathpati, C.; Vasanthakumaran, S.; Jain, D.; Hussain, Z.; Patel, S.; More, V. Light-Weight Thermal Insulating Fly Ash Cenosphere Ceramics. *Int. J. Appl. Ceram. Technol.* **2018**, *15*, 1467–1477. [CrossRef]
30. Hanif, A.; Diao, S.; Lu, Z.; Fan, T.; Li, Z. Green Lightweight Cementitious Composite Incorporating Aerogels and Fly Ash Cenospheres—Mechanical and Thermal Insulating Properties. *Constr. Build. Mater.* **2016**, *116*, 422–430. [CrossRef]
31. Haustein, E.; Kuryłowicz-Cudowska, A. The Effect of Fly Ash Microspheres on the Pore Structure of Concrete. *Minerals* **2020**, *10*, 58. [CrossRef]
32. Pundienė, I.; Pranckevičienė, J.; Kligys, M.; Kairitė, A.; Girskas, G. Effect of Adding Cenospheres on Heat-Resistant Lightweight Concrete Properties. *Refract. Ind. Ceram.* **2019**, *59*, 482–487. [CrossRef]
33. Huang, Z.; Padmaja, K.; Li, S.; Liew, J.Y.R. Mechanical Properties and Microstructure of Ultra-Lightweight Cement Composites with Fly Ash Cenospheres after Exposure to High Temperatures. *Constr. Build. Mater.* **2018**, *164*, 760–774. [CrossRef]
34. Rheinheimer, V.; Wu, Y.; Wu, T.; Celik, K.; Wang, J.; De Lorenzis, L.; Wriggers, P.; Zhang, M.H.; Monteiro, P.J.M. Multi-Scale Study of High-Strength Low-Thermal-Conductivity Cement Composites Containing Cenospheres. *Cem. Concr. Compos.* **2017**, *80*, 91–103. [CrossRef]
35. Zhou, H.; Brooks, A.L. Thermal and Mechanical Properties of Structural Lightweight Concrete Containing Lightweight Aggregates and Fly-Ash Cenospheres. *Constr. Build. Mater.* **2019**, *198*, 512–526. [CrossRef]
36. Gupta, S.; Kua, H.W. Application of Rice Husk Biochar as Filler in Cenosphere Modified Mortar: Preparation, Characterization and Performance under Elevated Temperature. *Constr. Build. Mater.* **2020**, *253*, 119083. [CrossRef]
37. Zhang, Y.; Xia, W. Enhancing Effect of Carbon Nanotubes on the Performance of Concrete Containing Surface-Treated Fly Ash Cenosphere. *Constr. Build. Mater.* **2023**, *406*, 133322. [CrossRef]
38. Kabay, N.; Aköz, F. Effect of Prewetting Methods on Some Fresh and Hardened Properties of Concrete with Pumice Aggregate. *Cem. Concr. Compos.* **2012**, *34*, 503–507. [CrossRef]
39. Kucharczyková, B.; Keršner, Z.; Pospíchal, O.; Misák, P.; Daněk, P.; Schmid, P. The Porous Aggregate Pre-Soaking in Relation to the Freeze–Thaw Resistance of Lightweight Aggregate Concrete. *Constr. Build. Mater.* **2012**, *30*, 761–766. [CrossRef]
40. Liu, Y.; Wei, Y. Internal Curing Efficiency and Key Properties of UHPC Influenced by Dry or Prewetted Calcined Bauxite Aggregate with Different Particle Size. *Constr. Build. Mater.* **2021**, *312*, 125406. [CrossRef]
41. Mora-Ortiz, R.S.; Del Angel-Meraz, E.; Díaz, S.A.; Magaña-Hernández, F.; Munguía-Balvanera, E.; Pantoja Castro, M.A.; Alavez-Ramírez, J.; Quiroga, L.A. Effect of Pre-Wetting Recycled Mortar Aggregate on the Mechanical Properties of Masonry Mortar. *Materials* **2021**, *14*, 1547. [CrossRef] [PubMed]
42. Ding, Q.; Xiang, W.; Zhang, G.; Hu, C. Effect of Pre-Wetting Lightweight Aggregates on the Mechanical Performances and Microstructure of Cement Pastes. *J. Wuhan Univ. Technol.-Mater. Sci. Ed.* **2020**, *35*, 140–146. [CrossRef]
43. Ji, T.; Zheng, D.D.; Chen, X.F.; Lin, X.J.; Wu, H.C. Effect of Prewetting Degree of Ceramsite on the Early-Age Autogenous Shrinkage of Lightweight Aggregate Concrete. *Constr. Build. Mater.* **2015**, *98*, 102–111. [CrossRef]
44. Chen, P.; Wang, J.; Liu, F.; Qian, X.; Xu, Y.; Li, J. Converting Hollow Fly Ash into Admixture Carrier for Concrete. *Constr. Build. Mater.* **2018**, *159*, 431–439. [CrossRef]
45. Jiawei, Z.; Wei, H.; Dajian, H.; Xuhui, L.; Jianhu, M.; Yong, Z.; Jiawei, Z.; Wei, H.; Dajian, H.; Xuhui, L.; et al. Preparation of Phase Change Microcapsules Based on Microporous Fly-Ash Cenosphere and Its Effect on the Mechanical and Thermal Properties of Mortar. *Acta Mater. Compos. Sin.* **2023**, *40*, 4703–4719. [CrossRef]
46. *EN 14647:2005/AC:2006*; Calcium Aluminate Cement-Composition, Specifications and Conformity Criteria. European Committee for Standardization: Brussels, Belgium, 2006.
47. Alcoa Industrial Chemicals. *Calcium Aluminate Cement. Test Methods*; Almatis GmbH: Frankfurt, Germany, 1999.
48. Pundienė, I.; Pranckevičienė, J.; Zhu, C.; Kligys, M. The Role of Temperature and Activator Solution Molarity on the Viscosity and Hard Structure Formation of Geopolymer Pastes. *Constr. Build. Mater.* **2021**, *272*, 121661. [CrossRef]
49. *EN ISO 1927-1:2012*; Monolithic (Unshaped) Refractory Products. European Committee for Standardization: Brussels, Belgium, 2012.
50. *EN 12390-3:2019*; Testing Hardened Concrete—Part 3: Compressive Strength of Test Specimens. European Committee for Standardization: Brussels, Belgium, 2019.
51. Fomenko, E.V.; Anshits, N.N.; Solovyov, L.A.; Mikhaylova, O.A.; Anshits, A.G. Composition and Morphology of Fly Ash Cenospheres Produced from the Combustion of Kuznetsk Coal. *Energy Fuels* **2013**, *27*, 5440–5448. [CrossRef]
52. Robeyst, N.; Gruyaert, E.; Grosse, C.U.; De Belie, N. Monitoring the Setting of Concrete Containing Blast-Furnace Slag by Measuring the Ultrasonic p-Wave Velocity. *Cem. Concr. Res.* **2008**, *38*, 1169–1176. [CrossRef]
53. Sarkar, R.; Samant, A.D. Study on the Effect of Deflocculant Variation in High-Alumina Low-Cement Castable. *Interceram-Int. Ceram. Rev.* **2016**, *65*, 28–34. [CrossRef]

54. Xia, Z.; Huang, W.; Zhang, J.; Li, X.; Wang, R.; Zhang, F.; Yu, B. Internal Curing of High Strength Concrete Based on Saturated Microporous Cenospheres. *Case Stud. Constr. Mater.* **2024**, *20*, e03072. [CrossRef]
55. Kudžma, A.; Stonys, R.; Antonovič, V. Influence of Nanographene Oxide on Calcium Aluminate Cement Hydration. *Interceram-Int. Ceram. Rev.* **2019**, *68*, 30–34. [CrossRef]
56. Sun, Y.; Wang, Z.H.; Park, D.J.; Kim, W.S.; Kim, H.S.; Yan, S.R.; Lee, H.S. Analysis of the Isothermal Hydration Heat of Cement Paste Containing Mechanically Activated Fly Ash. *Thermochim. Acta* **2022**, *715*, 179273. [CrossRef]
57. Hou, P.; Kawashima, S.; Kong, D.; Corr, D.J.; Qian, J.; Shah, S.P. Modification Effects of Colloidal NanoSiO2 on Cement Hydration and Its Gel Property. *Compos. Part B Eng.* **2013**, *45*, 440–448. [CrossRef]
58. Giergiczny, Z. Fly Ash and Slag. *Cem. Concr. Res.* **2019**, *124*, 105826. [CrossRef]
59. Akmalaiuly, K.; Berdikul, N.; Pundienė, I.; Pranckevičienė, J. The Effect of Mechanical Activation of Fly Ash on Cement-Based Materials Hydration and Hardened State Properties. *Materials* **2023**, *16*, 2959. [CrossRef] [PubMed]
60. Okino, E.Y.A.; De Souza, M.R.; Santana, M.A.E.; Alves, M.V.D.S.; De Sousa, M.E.; Teixeira, D.E. Cement-Bonded Wood Particleboard with a Mixture of Eucalypt and Rubberwood. *Cem. Concr. Compos.* **2004**, *26*, 729–734. [CrossRef]
61. Sikora, P.; Łukowski, P.; Cendrowski, K.; Horszczaruk, E.; Mijowska, E. The Effect of Nanosilica on the Mechanical Properties of Polymer-Cement Composites (PCC). *Procedia Eng.* **2015**, *108*, 139–145. [CrossRef]
62. Oumarou, N.; Kocaefe, D.; Kocaefe, Y. Investigation of the Refractory Bricks Used for the Flue Wall of the Horizontal Anode Baking Ring Furnace. *Ceram. Int.* **2016**, *42*, 18436–18442. [CrossRef]
63. Otroj, S.; Nilforoushan, M.R.; Reza, M. The Effect of Additives on the Properties of High Alumina Low-Cement Self-Flowing Castables. *Ceram.-Silik.* **2009**, *53*, 42–47.
64. Solanki, A.; Singh, L.P.; Karade, S.R.; Sharma, U. Functionality of Silica Nanoparticles on Hydration Mechanism and Microstructure of Tricalcium Aluminate. *Constr. Build. Mater.* **2021**, *299*, 124238. [CrossRef]
65. Pundiene, I.; Pranckeviciene, J.; Kligys, M. Effect of a Mixture of Different Types of Deflocculants on the Structure and Properties of Cement Rock and Castable Refractories. *Glas. Ceram.* **2017**, *74*, 295–301. [CrossRef]
66. Sarkar, R. Binders for Refractory Castables: An Overview. *Interceram-Int. Ceram. Rev.* **2020**, *69*, 44–53. [CrossRef]
67. Traoré, K.; Kabré, T.S.; Blanchart, P. Gehlenite and Anorthite Crystallisation from Kaolinite and Calcite Mix. *Ceram. Int.* **2003**, *29*, 377–383. [CrossRef]
68. Kearney, S.; Yorkshire, A.S.; Geddes, D.A.; Hanein, T.; Nelson, S.; Provis, J.L.; Walkley, B. Cement-Based Stabilization/Solidification of Radioactive Waste. In *Low Carbon Stabilization and Solidification of Hazardous Wastes*; Elsevier: Amsterdam, The Netherlands, 2022; pp. 407–431. [CrossRef]
69. Bouhifd, M.A.; Gruener, G.; Mysen, B.O.; Richet, P. Premelting and Calcium Mobility in Gehlenite ($Ca_2Al_2SiO_7$) and Pseudowollastonite ($CaSiO_3$). *Phys. Chem. Miner.* **2002**, *29*, 655–662. [CrossRef]
70. Mysen, B.O. Energetics of Melts and Melting in Magmatic Systems. In *Mass Transport in Magmatic Systems*; Elsevier: Amsterdam, The Netherlands, 2023; pp. 213–274. [CrossRef]
71. Cheriton, L.W.; Gupta, J.P. Building Materials. In *Encyclopedia of Analytical Science*, 2nd ed.; Elsevier: Amsterdam, The Netherlands, 2005; pp. 304–314. [CrossRef]
72. Goldsmith, J.R. The Melting and Breakdown Reactions of Anorthite at High Pressures and Temperature. *Am. Mineral.* **1980**, *65*, 272–284.
73. Schoneveld, L.; O'Neill, H.S.C. The Influence of Melt Composition on the Partitioning of Trace Elements between Anorthite and Silicate Melt. *Contrib. Miner. Petrol.* **2019**, *174*, 13. [CrossRef]

Disclaimer/Publisher's Note: The statements, opinions and data contained in all publications are solely those of the individual author(s) and contributor(s) and not of MDPI and/or the editor(s). MDPI and/or the editor(s) disclaim responsibility for any injury to people or property resulting from any ideas, methods, instructions or products referred to in the content.